Tertiary creep stage in a non linear kinematics and isotropic hardening elasto-visco-plastic model.

MICHEL B.*, ASSIRE A.*, CAMBEFORT** P.

*DER/SERI/LFEA CEA de Cadarache 13108 St-Paul-lez-Durance FRANCE
**EDF/SEPTEN 12-14, Avenue Dutrievoz 69628 VILLEURBANNE CEDEX France

ABSTRACT:

The aim of the present paper is to introduce tertiary creep stage phenomenon in an elasto-visco-plastic model taking into account primary and secondary creep stages. The study is based on the "D.D.I. (Two Inelastic Strains)" model [2], in which an elasto-plastic and a visco-plastic potentials are used to describe material behaviour under cyclic loading with dwell periods at high temperature. Creep phenomenon are described with the visco-plastic part of the model, using a non linear kinematic hardening with a recovery time effect. Experimental data used to analyse the tertiary creep stage in weld metal are deduced from six creep tests at 600°C.

A pseudo analytical procedure is proposed to identify tertiary creep parameters in the Two Inelastic Strains Model. Simulation at different stress levels shows that tertiary creep strain assessment is in good agreement with experimental results.

INTRODUCTION :

The industrial context of this study concerns life time assessment of austenitic stainless steel welded junctions in high temperature components. In order to best estimate stress and strain fields in the welded joint a detailed description of weld and base metals behaviour is needed. As austenitic stainless steel weld metals can present a significant tertiary creep stage (half of the time to rupture) the aim of this paper is to introduce this phenomenon in constitutive equations of an elasto-visco-plastic model. Our study will focus on an austeno-ferritic weld metal with 19% Cr, 12% Ni and 2% Mo, for which tertiary creep stage doesn't seem to be only linked to a damage effect, but also to a metallurgical transformation phenomenon. Constitutive equations are based on the "DDI (Two Inelastic Strains)" model [2] where an elasto-plastic and a visco-plastic potential are used to take into account cyclic loading with dwell period at high temperature.

The present paper will be divided in three parts. First the microstructure of the studied weld metal will be presented. In a second part, a phenomenological and a metallurgical descriptions of tertiary creep stage will be proposed with experimental results of six tensile tests. Finally, a modification of the visco-plastic law in the DDI model will be discussed in order to take into account primary, secondary and tertiary creep stages.

WELD METAL MICROSTRUCTURE :

The chemical composition of the studied weld metal (NERTALINOX) is presented in Table 1. In the latter we can see that this weld metal is similar to the OKR3U austeno-ferritic weld metal used in French Fast Breeder Reactors. Both weld metal have a 316L type chemical composition. Microstructure of 316L type weld metal is shown on Figure 1 extracted from reference [1]. This is a two phases microstructure with an austenitic matrix and clusters of thin ferrite dendrites. The austenitic matrix is made of columnar grains 50 microns large and 1 or 2 mm long. The orientation of columnar grains, linked to the solidification process, is given by the TC axe as shown on Figure 1. The oriented microstructure lead to an anisotropic behaviour. How ever, in order to simplify constitutive modelling, creep tensile properties will be characterized only in the "Transverse direction" (T on Figure 1), which is the main loading axis in a welded junction.

Table 1 : Weld metal chemical compositions

	C	S	P	Si	Mn	Cr	Ni	Mo	Teneur en ferrite Méthode	δ%
OKR3U Rapsodie	0.050 0.065	-	-	0.50-0.80	1.2-1.5	18.0-19.0	11.0-12.0	1.9-2.2		< 5
OKR3U Phénix	< 0.040	< 0.025	< 0.030	0.40-0.80	1.2-2.0	18.0-19.0	11.5-13.0	1.8-2.2	MMS	< 5
**	0.045 0.055	S+P < 0.030		0.30-0.50	1.0-1.5	19.0-19.5	11.0-11.5	1.8-2.2	MMS	< 5
OKR3U Super Phénix	0.045 0.055	< 0.020	< 0.025	0.40-0.70	1.2-1.8	18.0-19.0	11.0-12.0	1.9-2.2	MMS	3-7
Nertalinox	0.012			0.40	1.5	19.0	12.5	2.5		

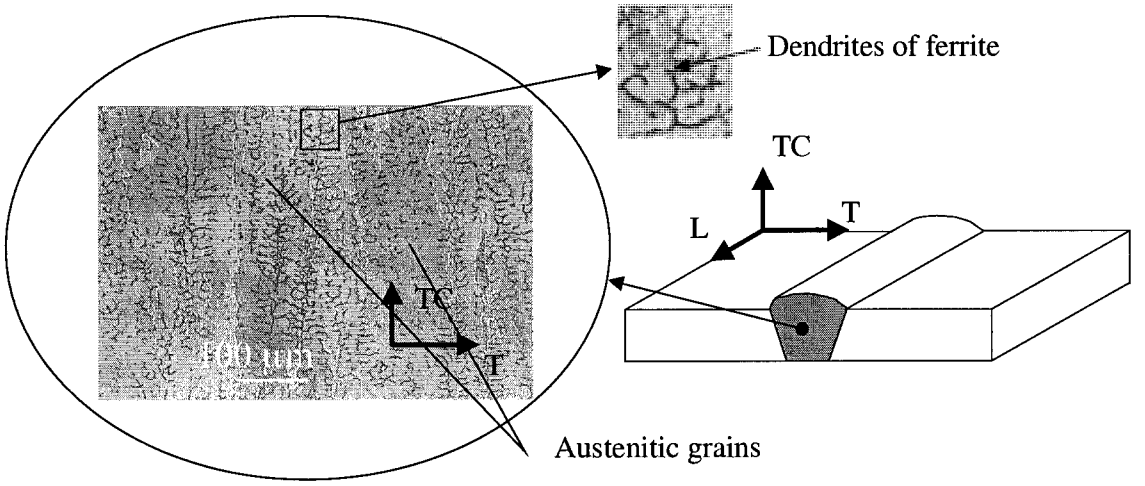

Figure 1 : 316L type weld metal microstructure

TERTIARY CREEP STAGE :

To identify tertiary creep stage six tests have been carried out on weld metal tensile specimens extracted from a mould as shown on Figure 2. Creep tensile test experimental results for a stress level range from 210 MPa up to 275 MPa are presented on Figure 3.

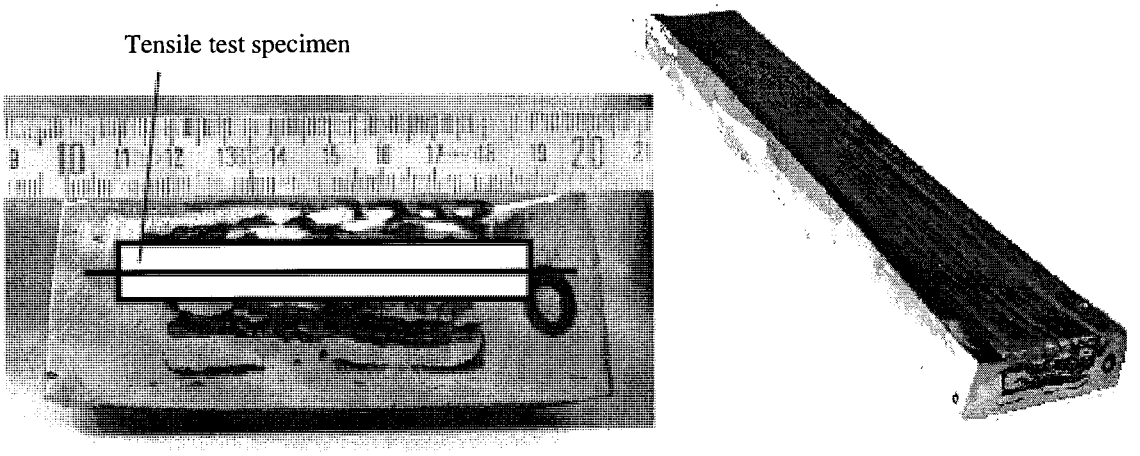

Figure 2 : NERTALINOX weld metal mould

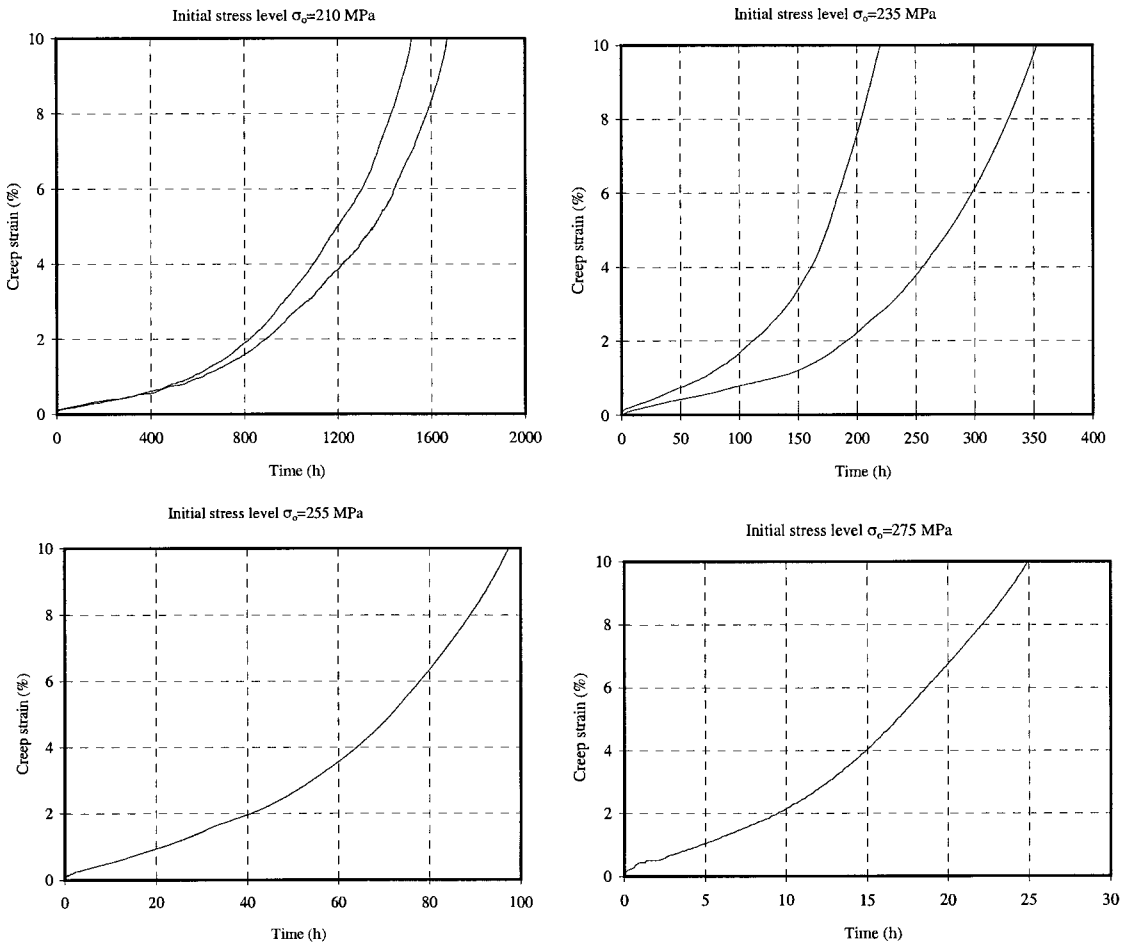

Figure 3 : Tensile creep tests on NERTALINOX weld metal at 600°C

As we can see on Figure 3 tertiary creep stage represents at least half of the time to rupture and start at a low creep strain level. Actually, the end of secondary creep stage approximately occurred at 1% of creep strain for each stress level. This last remark leads us to conclude that tertiary creep stage beginning is strongly linked to the cumulated creep strain.

Tertiary creep stage in weld metal is a competition between following phenomena :

- large displacement and localisation
- damage cavitations at grain boundaries
- metallurgical transformation

Concerning the first point, if we solve the tensile creep problem with a secondary creep law taking into account the uniform section area reduction (Figure 4) we can see that the true stress increase is not important enough to explain a significant tertiary creep stage at 1% or 2% of creep strain. Moreover, localisation doesn't occurred for such low strain levels. In our case we will choose to identify tertiary creep stage with a conventional approach (small displacement theory), in order to maximize creep strain in predictive computations.

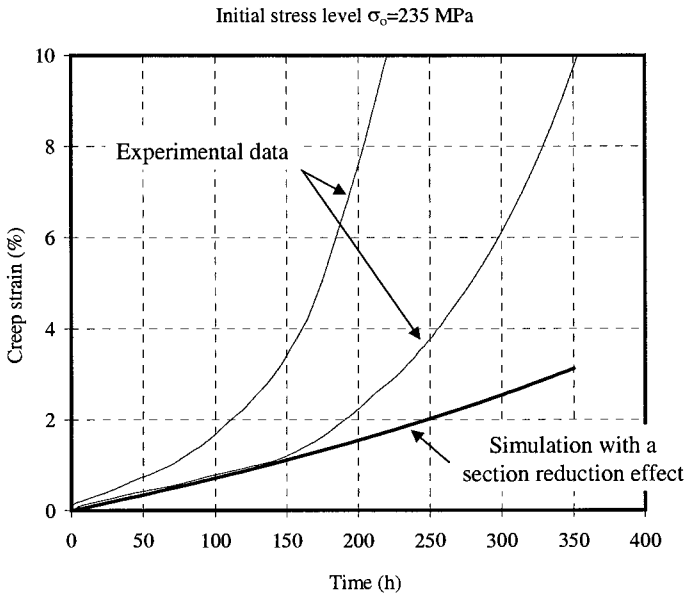

Figure 4 : Section reduction effect in the tertiary creep stage

Creep damage cavitations in 316L type weld metals have been studied in reference [1]. In the latter it's not obvious that damage cavitations have a significant contribution at the beginning of tertiary creep stage. Actually, intergranular void fraction observed for low creep strain levels is very small, and has probably a negligible effect on the effective stress.

Concerning metallurgical transformation, chromium carbide precipitation is invoked in reference [1] to explain a decreasing proportion of carbon in the austenitic matrix, inducing a softening effect on the weld metal. This third point could have a major contribution in tertiary creep stage at low strain level. As experimental results show that tertiary creep stage starts at 1% of creep strain in a dwell period range of 10 to 500 hours, we can think that the kinetic of chromium carbide precipitation is strongly correlated to creep strain rate.

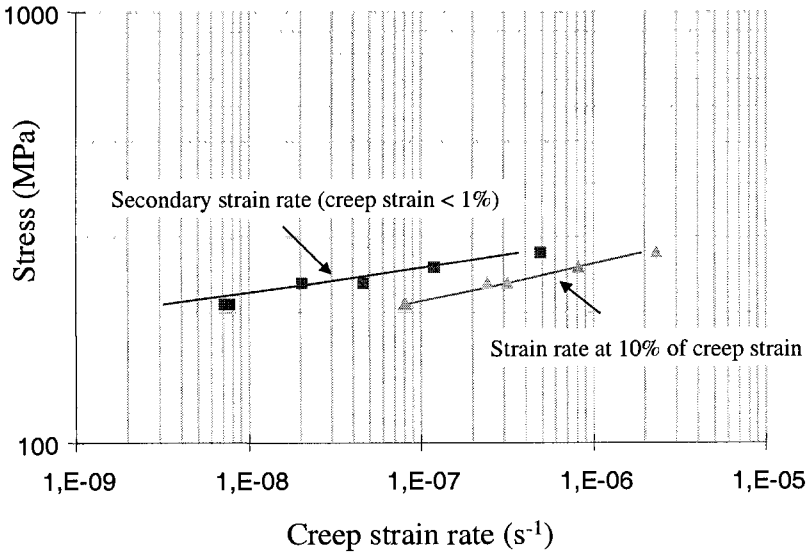

Figure 5 : Strain rate increase during tertiary creep stage

On Figure 5 creep strain rate as a function of stress is represented for different creep strain levels. As we can see, creep strain rate is a power law function of the stress even during tertiary stage. According to these results we assume that tertiary creep strain rate can be derived from a Norton power law with a set of coefficients function of the cumulated creep strain.

TWO INELASTIC STRAIN MODEL (DDI).

Constitutive equations

Table 2 : Constitutive equations of the DDI model

Inelastic strain decomposition	
$\underline{\underline{\varepsilon}}_{total} = \underline{\underline{\varepsilon}}_{elastic} + \underline{\underline{\varepsilon}}_{plastic} + \underline{\underline{\varepsilon}}_{viscoplastic}$ (1)	
non time dependant strain	time dependant strain
Yield functions	
$f_p = J\left(\underline{\underline{\sigma}} - \underline{\underline{X_p}}\right) - R_p$ (2)	$f_v = J\left(\underline{\underline{\sigma}} - \underline{\underline{X_v}}\right) - R_V$ (11)
plastic strain rate	visco-plastic strain rate
$\dot{\lambda}_p = \dot{p} = \left\langle \frac{\dot{\underline{\underline{\sigma}}} : \underline{\underline{n_p}} - \frac{2}{3} c_{vp} \cdot \dot{\underline{\underline{\alpha}}}_v : \underline{\underline{n_p}}}{H} \right\rangle$ (3) où : $H = c_p \left(\frac{d_p}{c_p} - \underline{\underline{X_p}} : \underline{\underline{n_p}} \right) + b_p \left(R_{P_0} + Q_p - R_p \right)$ (4)	$\dot{\lambda}_v = \dot{v} = \left\langle \frac{J\left(\underline{\underline{\sigma}} - \underline{\underline{X_v}}\right) - R_v}{K(v)} \right\rangle^{n(v)}$ (12) tertiary creep : $n(v) = A_n \cdot (v)^{n'} + B_n$ (13) $K(v) = A_K \cdot v + B_K$ (14)
isotropic hardening	
$R_P = R_{P_0} + Q_P \cdot \left(1 - e^{-b_P \cdot p}\right) + Q'_P \cdot \left(1 - e^{-b'_P \cdot p}\right)$ (5)	$R_v = R_{v_0} + Q_v \left(1 - e^{-b_v \cdot v}\right)$ (15)
non linear kinematics hardening for plastic parameters	
$\varphi_C(p) = \varphi_{C_S} + (1 - \varphi_{C_S}).e^{-\omega.p}$ (6)	$\varphi_D(p) = \varphi_{D_S} + (1 - \varphi_{D_S}).e^{-\omega.p}$ (16)
$\underline{\underline{X_{P_1}}} = \frac{2}{3} c_{P_1} \cdot \underline{\underline{\alpha_{P_1}}} + \frac{2}{3} c_{VP_1} \cdot \underline{\underline{\alpha_{V_1}}}$ (7)	$\dot{\underline{\underline{\alpha}}}_{P_1} = \dot{\underline{\underline{\varepsilon}}}_P - \frac{3}{2} \frac{d_{P_1}}{c_{P_1}} \cdot \underline{\underline{X_{P_1}}} \cdot \dot{p}$ (17)
$\underline{\underline{X_{P_2}}} = \frac{2}{3} c_{P_2} \cdot \varphi_C(p) \cdot \underline{\underline{\alpha_{P_2}}} + \frac{2}{3} c_{VP_2} \cdot \underline{\underline{\alpha_{V_2}}}$ (8)	$\dot{\underline{\underline{\alpha}}}_{P_2} = \dot{\underline{\underline{\varepsilon}}}_P - \frac{3}{2} \frac{d_{P_2} \cdot \varphi_D(p)}{c_{P_2} \cdot \varphi_C(p)} \cdot \underline{\underline{X_{P_2}}} \cdot \dot{p}$ (18)
non linear kinematics hardening for visco- plastic parameters	
$\underline{\underline{X_{V_1}}} = \frac{2}{3} c_{V_1} \cdot \underline{\underline{\alpha_{V_1}}} + \frac{2}{3} c_{VP_1} \cdot \underline{\underline{\alpha_{P_1}}}$ (9)	$\dot{\underline{\underline{\alpha}}}_{V_1} = \dot{\underline{\underline{\varepsilon}}}_V - \frac{3}{2} \frac{d_{V_1}}{c_{V_1}} \cdot \underline{\underline{X_{V_1}}} \cdot \dot{v} - \left(\frac{\left\lvert \underline{\underline{X_{V_1}}} \right\rvert}{M} \right)^m \cdot \frac{\underline{\underline{X_{V_1}}}}{\left\lvert \underline{\underline{X_{V_1}}} \right\rvert}$ (19)
$\underline{\underline{X_{V_2}}} = \frac{2}{3} c_{V_2} \cdot \underline{\underline{\alpha_{V_2}}} + \frac{2}{3} c_{VP_2} \cdot \underline{\underline{\alpha_{P_2}}}$ (10)	$\dot{\underline{\underline{\alpha}}}_{V_2} = \dot{\underline{\underline{\varepsilon}}}_V - \frac{3}{2} \frac{d_{V_2}}{c_{V_2}} \cdot \underline{\underline{X_{V_2}}} \cdot \dot{v}$ (20)

The total strain in the two inelastic strain model (DDI) [2] is derived from equation (1) in Table 2. Inelastic strains are computed with two non linear kinematic and isotropic hardening models respectively associated to an elasto-plastic and a visco-plastic potential. Constitutive equations of the model used in our study [3] are presented in Table 2. An identification of this model for the NERTALINOX weld metal at 600°C is proposed in Table 3. Concerning the plastic part of the model some modifications have been proposed in our study compared to the previous version of the DDI model used in reference [2]. First a softening effect has been included in the plastic isotropic variable R_p (5). This phenomenon is specific to the behaviour of the weld metal, where cyclic response of the material show a hardening effect for the first cycles and then a softening effect non stabilized until rupture. A second modification has been proposed with strain dependant kinematic parameters in equations (6) and (16). The latter enables to best estimate the difference between monotonic and cyclic consolidation curve shapes. This phenomenon is more significant in the base metal than in the weld metal. Coefficients φ_C and φ_D in Equations (6) and (16) are used to modify kinematics parameters C_{P2} and D_{P2} when the material response is stabilized. The only kinematic variable concerned by this modification (X_{p2} in our case) is the one used to represent kinematic hardening at the beginning of plasticity (plastic strain lower than 1%).

Primary and secondary creep stage parameters identification

In reference [3] a pseudo analytical procedure has been developed for the identification of plastic and visco-plastic parameters. In order to simplify the problem, coupling parameters c_{vp1}, c_{vp2} are not taken into account. With this hypothesis we assume that the plastic and the viscoplastic parts of the model are respectively dedicated to time none dependent and time dependant strains with no interaction. For austenitic stainless steels and their weld metals these two behaviours can be approximately associated to high strain rates ($> 10^{-6}$ s^{-1}) and low strain rates ($< 10^{-8}$ s^{-1}) as shown on Figure 6. Therefore, plastic parameters are identified with monotonic and cyclic tensile tests at a strain rate of 10^{-3} s^{-1}, and visco-plastic parameters will be identified with creep or relaxation tests with lower strain rates. For austenitic stainless steels the physical meaning of this strain partitioning can be attributed to the "Portevin-Le Châtelier" phenomenon as described in [2]. In this paper, only the analytical procedure to identify visco-plastic parameters will be described, more details concerning plastic parameters are available in references [3] and [4].

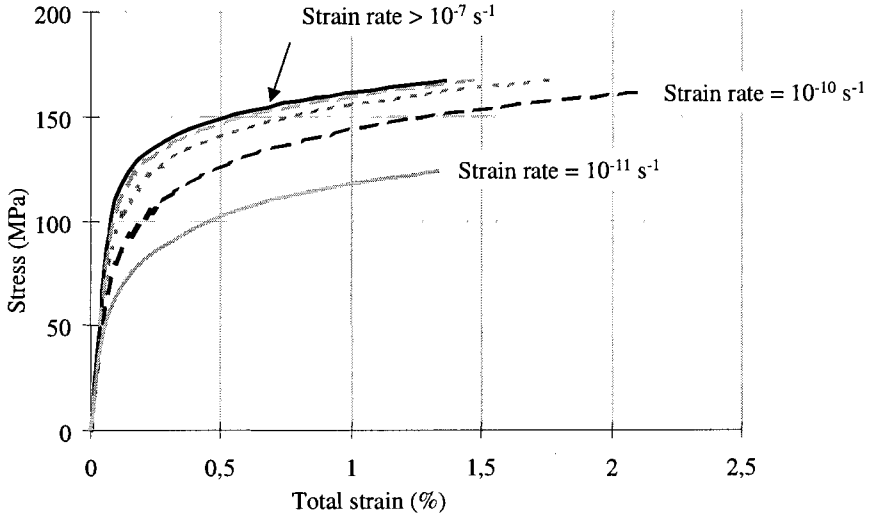

Figure 6 : Strain rate hardening sensitivity for austenitic stainless steel 316L (N)

As there is no significant yield effect on creep strain for austenitic stainless steels at 600°C, the isotropic hardening is avoided in the visco plastic model. Then visco plastic strain rate equation is simplified and becomes :

$$\dot{v} = \left\langle \frac{J(\underline{\underline{\sigma}} - \underline{\underline{X}}_v)}{K(v)} \right\rangle^{n(v)} \tag{21}$$

In order to have a power law relationship between visco plastic strain rate and stress (Figure 5) during secondary creep stage, we assume that the asymptotic value of the kinematic variable is a linear function of the applied stress :

$$\underline{\underline{X}}_v^{\text{asymptotic}} = a.\underline{\underline{\sigma}} \Rightarrow \dot{v} = \left\langle \frac{(1-a).J(\underline{\underline{\sigma}})}{K(v)} \right\rangle^{n(v)} \tag{22}$$

An easy identification of parameters K(v), n(v) and a can be derived from equation (22) and experimental data of the secondary creep law (Figure 5) with the following step by step procedure :

- the parameter n is equal to the exponent of the secondary creep law
- set the parameter K in order to have an initial creep strain rate ($X_v = 0$) representative of the primary stage
- set the parameter "a" solving equation (23)

$$C_s.J(\underline{\underline{\sigma}})^{n_s} = \left\langle \frac{(1-a).J(\underline{\underline{\sigma}})}{K} \right\rangle^{n_s} \tag{23}$$

Where C_s and n_s are the secondary creep law parameters

Parameters K(v) and n(v) are constant during primary and secondary creep stages. Visco-plastic kinematics parameters are then identified with the experimental value of "a" by solving equation (24). To solve the latter it's no use to have a differential solver because the asymptotic problem can be formulated as a non linear equation.

$$\underline{\underline{X}}_v^{\text{asymptotic}} = a.\underline{\underline{\sigma}} \tag{24}$$

This analytical procedure has been used to identify the DDI model on primary and secondary creep stages (see Table 3) of six tests presented on Figure 3. As we can see on Figure 7 simulations are in good agreement with experimental results for a large range of stress levels.

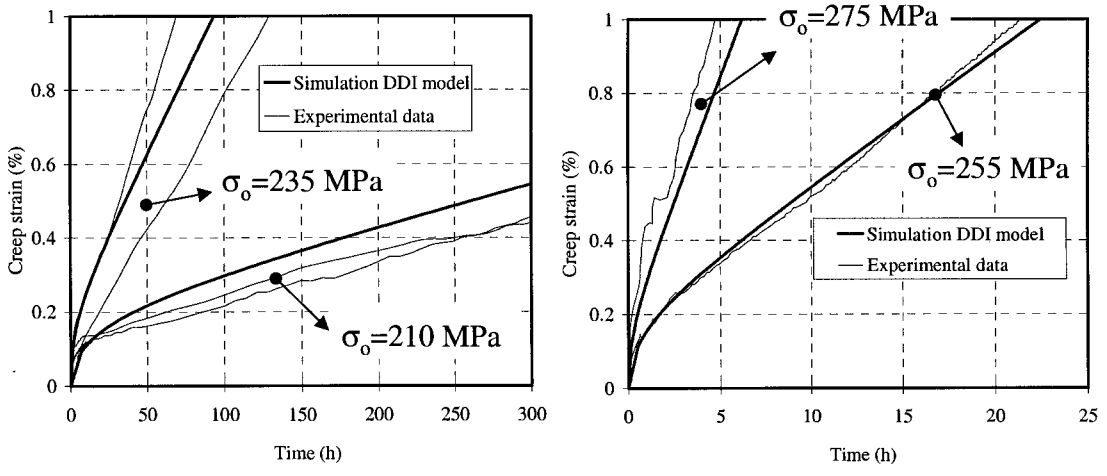

Figure 7 : Primary and secondary creep stages simulation with the DDI model

Table 3 : DDI model parameters for NERTALINOX weld metal at 600°C (stress : MPa, strain rate : s^{-1})

E	ν	Rp_0	Qp	bp	Q'p	b'p	cp_1	dp_1	cp_2	dp_2
145000	0,3	200	-30	0,6	0	0	2108	10,4	167837	2133
φ_{Cs}	$\varphi_{\Delta\sigma}$	w	Rv_0	Qv	bv	cv_1	dv_1	cv_2	dv_2	M
0,18	0,09	0,6	0	20	10	0	0	250000	2500	0
m	K	n	K_{final}	n_{final}	$v_{initial}$	v_{final}	cvp_1	cvp_2		
0	571	12,47	571	12,47	0,01	0,1	0	0		

Tertiary creep stage parameters identification

As presented on Figure 5 tertiary creep stage is identified via the strain rate increase being a function of cumulated creep strain. Therefore parameters of the strain rate-stress power law are creep strain dependent after the end of the secondary creep stage. In order to be consistent with the analytical procedure of paragraph 4.2. parameters K(v) and n(v) are identified by solving equation (25) with the previous value of "a" given by primary and secondary creep stages.

$$C_t.J(\underline{\underline{\sigma}})^{n_t} = \left\langle \frac{(1-a).J(\underline{\underline{\sigma}})}{K(v)} \right\rangle^{n(v)} \tag{25}$$

Where C_t and n_t are creep strain dependant parameters of the tertiary creep law.

K(v) and n(v) optimal values obtained for tertiary creep stages of the six creep tensile tests presented on Figure 3 are plotted on Figure 8. Discrete values of K(v) and n(v) are respectively fitted with linear and power functions (14) and (13) in Table 2.

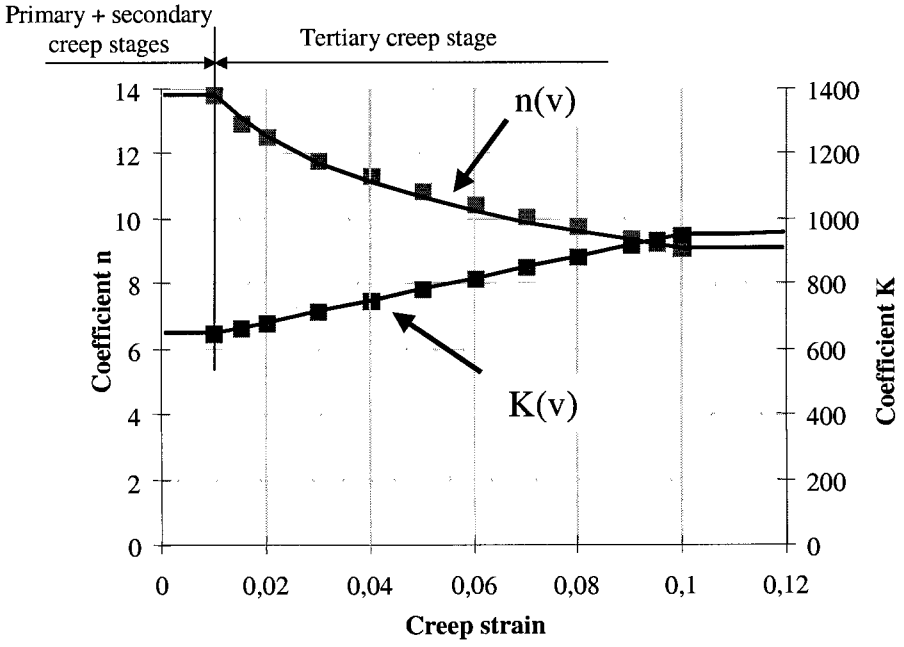

Figure 8 : Identification of parameters K(v) and n(v) during tertiary creep stage.

A simulation of the tertiary creep stage with parameters K(v) and n(v) identified on Figure 8 is presented on Figure 9. Simulations are still in good agreement with experimental results for a large range of stress levels. To avoid numerical

problems we consider that visco-plastic strain rate is constant for cumulated creep strain greater than 10%. Anyway, our identification is no more valid for such strains.

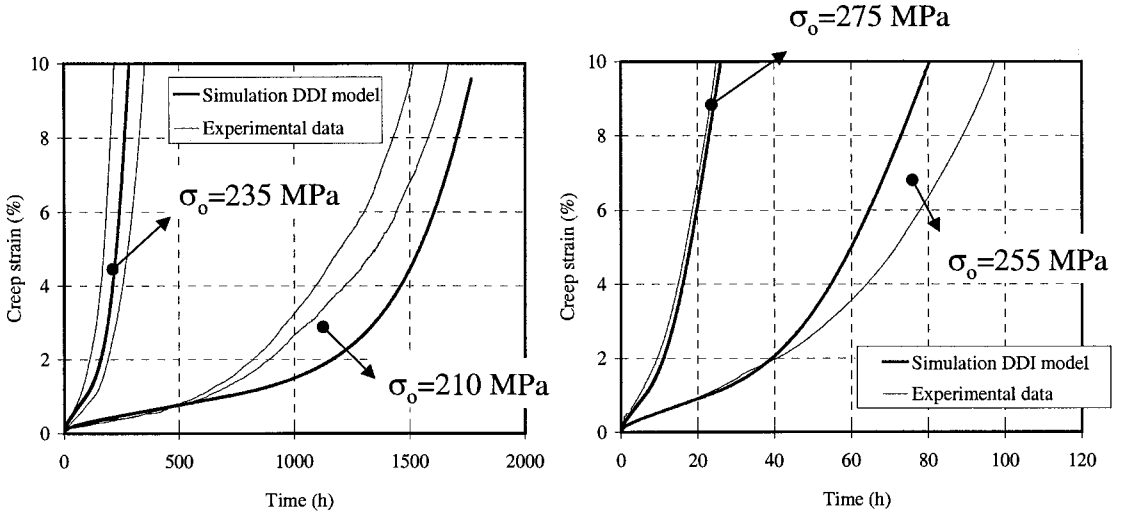

Figure 9 : Tertiary creep stage simulation with the DDI model

DISCUSSION

As high temperature intergranular fracture can occurred for few percents of creep strain our study was limited to low strain level assessment. The main objective was to best estimate the beginning of tertiary creep stage occurring in 316L type weld metal. As presented in paragraph 3 tertiary creep stage at low strain level seems to be mainly due to chromium carbide precipitation. As damage cavitations doesn't seem to be responsible of tertiary creep stage in our case, models using coupling damage approach have been avoided. Moreover a conventional approach, based on small displacement theory, has been chosen to identify tertiary creep stage in order to over estimate creep strain in predictive assessments. Of course it could be interesting to have a rational approach at the identification stage, however we have to be aware that this could lead to unsafe assessments if localisation phenomenon are not well detected. Moreover a detailed Finite Element analysis is needed to distinguish the part due to large displacements in the tertiary global response of a creep tensile test. Therefore tertiary creep stage has been identified with a phenomenological approach. The latter consisting to introduce creep strain dependant parameters in the viscoplastic potential of a two inelastic strain model. This approach has been used, rather than introducing new state variables, in order to minimize model modifications and to provide an easy identification procedure of tertiary creep stage parameters. Indeed, the analytical identification procedure developed for secondary creep stage can be used without any modification.

CONCLUSIONS

Tertiary creep stage in austenitic stainless steel (316L type) weld metals has been studied. Experimental results of creep tensile tests show a significant tertiary creep stage with a secondary creep stage end at about 1% of cumulated creep strain. A bibliographic analysis let us think that tertiary creep stage at low strain level is mainly due to chromium carbide precipitation, and that large displacement phenomenon and damage cavitations have a negligible contribution at the beginning.

A modification of the "Two Inelastic Strain" model has been proposed in order to take into account tertiary creep stage. The latter has been introduced via the two parameters K and n used in the Norton law of the visco-plastic potential. A pseudo analytical procedure used to identify primary, secondary and tertiary creep stages has been detailed. This step by step procedure gives a phenomenological justification of each parameter. A set of parameters for an identification on NERTALINOX weld metal at 600°C has been proposed. Simulations at different stress levels (from 210 MPa to 275 MPa) show that primary, secondary and tertiary creep strain assessments are in very good agreement with experimental results.

REFERENCES :

1. BOUCHE G. and al. "Modelling of microstructural creep damage in welded joints of 316L stainless steel", ECF12, Vol1, pp 357-362, Emas, Sept. 1998.

2. CONTESTI E. "Description of creep-plasticity interaction with non unified constitutive equations. application to an austenitic stainless steel", NED, 116, pp265-280,1989.

3. A. ASSIRE "Amorçage et propagation de la fissuration dans les jonctions soudées à haute température", Ph-D thesis, 2000.

4. A. ASSIRE and al. "Comportement d'aciers inoxydables à haute temperature pour les joints soudés", 4ème Colloque en Calcul des Structures, Giens, France, 1999.